THE EFFECTS OF PITTING ON FATIGUE CRACK NUCLEATION IN 7075-T6 ALUMINUM ALLOY

Li Ma and David W. Hoeppner *
University of Utah
Salt Lake City, UT

SUMMARY

A high-strength aluminum alloy, 7075-T6, was studied to quantitatively evaluate chemical pitting effects on its corrosion fatigue life. The study focused on pit nucleation, pit growth, and fatigue crack nucleation. Pitting corrosion fatigue experiments were conducted in 3.5% NaCl aqueous solution under constant amplitude sinusoidal loading at two frequencies, 5 and 20 Hz. Smooth and unnotched specimens were used in this investigation. A video recording system was developed to allow in situ observation of the surface changes of the specimens during testing. The results indicated that pitting corrosion considerably reduces the fatigue strength by accelerating fatigue crack nucleation.

A metallographic examination was conducted on the specimens to evaluate the nature of corrosion pits. First, the actual shapes of the corrosion pits were evaluated by cross-sectioning the pits. Secondly, the relation between corrosion pits and microstructure was also investigated. Finally, the possibility of another corrosion mechanism that might be involved in pitting was explored in this investigation.

The fractography of the tested specimens showed that corner corrosion pits were responsible for fatigue crack nucleation in the material due to the associated stress concentration. The pits exhibited variance of morphology. Fatigue life for the experimental conditions appeared to be strongly dependent on pitting kinetics and the crack nucleation stage.

INTRODUCTION

Pitting corrosion is a form of serious damage in aircraft structures, because aluminum alloys, particularly high-strength aluminum alloys used in aircraft structures, are susceptible to pitting when exposed to an aggressive environment. This is of importance, as aircraft often operate in aggressive environments. Many studies have been done on aluminum alloys dealing with this localized form of corrosion attack, such as determining the conditions that lead to pitting, how the basic mechanisms of pitting works, and developing effective methods of protection; however, little has been reported on the effects of pitting on the fatigue life of these alloys. Studies by Hoeppner [1,2] showed that pitting did have a significant effect on corrosion fatigue life. This study is an extension of this earlier work focusing on the pitting and crack nucleation stages of the work.

In recent years issues concerning the structural integrity and continued safe operation of aging aircraft have focused much attention on the effects of corrosion on the fatigue behavior of aircraft structural materials. Since high-strength aluminum alloy 7075-T6 is widely used in aircraft structures included in the aging fleet, it was believed important to study 7075-T6. Also, the conjoint action of corrosion pitting with fatigue loading lowers the overall structural integrity of those aircraft made of 7075-T6. This is oftentimes an extremely dangerous situation, as rapid failure without warning may occur under certain conditions. Thus, an extensive study on pitting corrosion fatigue behavior of this material is necessary.

In order to investigate the effects of pitting on the fatigue life of 7075-T6 aluminum alloy, the present work was mainly concerned with stages of pit nucleation and growth, and nucleation of fatigue cracks at

*This paper is based, in part, on the Ph.D. dissertation of the first author.

corrosion pit sites, because pitting corrosion was considered to have a more pronounced influence on the stage of crack nucleation in the overall fatigue process.

The primary objectives of this investigation were to develop a method for better understanding the role of pits in corrosion fatigue, and quantitatively assess pitting corrosion fatigue behavior of 7075-T6 aluminum alloy exposed to an aggressive environment.

EXPERIMENTS AND RESULTS

Experimental Procedures

Tests were conducted on 7075-T6 aluminum alloy. Typical mechanical properties and nominal composition (%wt) of the material are given in Tables 1 and 2 respectively.

The specimen used in this study was smooth and unnotched, and is shown in Fig. 1. The observed surface, which was the midsection of the upper surface of the specimen when mounted in the grips, was ground flat with 600-grit emery paper and cleaned with acetone before testing. The other surfaces including sides and bottom which could not be observed during testing, were coated with epoxy resin to isolate them from the corrosive solution.

The testing was conducted in a fretting fatigue machine which was modified for pitting corrosion fatigue tests. An environmental system was built to provide a flowing corrosive environment around the midsection of the specimen. A video recording system was developed to allow in situ observation of the specimen surface and real-time video recording. The use of this system permitted direct observation of transient surface changes without disturbing the reacting surface during the pitting corrosion fatigue testing. A schematic diagram of the system is shown in Fig. 2. Video images were produced using a microscope with a zoom lens fitted to a video camera. The microscope, which has two degrees of freedom, was positioned parallel to the specimen surface. Surface changes on the specimen during testing were monitored and recorded in real time by using the microscope, camera, VCR and monitor. A video micrometer was used for pit size and crack length measurement. A character generator was allowed to add titles or captions in the video images recorded and a video printer was used to produce permanent records of the images.

Seventeen unnotched specimens were tested in a 3.5% NaCl solution having pH values between 5 and 6. One specimen was tested in laboratory air for comparison. All tests were conducted at room temperature. In order to obtain fatigue lives of 10^6 to 10^7 cycles, the maximum stress levels used were varied between 79 MPa and 89 MPa. All specimens were tested under sinusoidal loading with a load ratio, R=0.1, at frequencies 5 and 20 Hz.

The fatigue load was applied after the specimen had been immersed in the 3.5% NaCl solution for a few minutes. The exposed areas of each specimen were the upper midsurface having areas of approximately 46 to 65 mm^2. The solution was circulated through the environmental chamber at a rate about 125mL/h. The solution was renewed for each test. Tests were not interrupted except for checking and cleaning the exposed surface, and taking photos.

Results and Discussion

Pit Nucleation

The pit size life in terms of number of cycles, plotted against the maximum stress level is shown in Fig. 3. Here, the pit detection life is defined as the number of cycles to the "first observed" pit at the length of about 0.02 mm on the exposed surface. Thus, the pit detection life includes the nucleation phase as well as some pit growth. It should be noted that fairly large scatter (between 9,52,800 and 2,621,300 cycles) in the pit detection life data was observed at both frequencies (5 and 20 Hz). This scatter is believed to be related to the distribution of constituent particles, inclusions, as well as grain shape, size, and orientation.

The data shown in Fig. 3 indicate that pitting generally was detected after approximately one million cycles. The reason for the delay in pit formation is that pitting corrosion is a time (or cycles) dependent process. It takes time for aggressive anions (Cl^-) contained in the solution to penetrate the passive film and locally destroy it. It was observed that, in 3.5% NaCl solution, the exposed surfaces of the specimens were corroded over whole areas in the very early stages of the test. Then corrosion pits were generated within the heavily corroded region. A typical series of video photographs showing the change in surface state of a specimen exposed to 3.5% NaCl solution are shown in Fig. 4. Within 68,900 cycles of exposure, the surface was obscured. The formation of a continuous corrosion product layer formed with progressive cycling, and the pits nucleated at localized attack sites. This observation is consistent with previous observation of Hoeppner[2] and Cox.[3]

One characteristic feature observed during the testing was the formation of blisters. These blisters occurred on the surface and burst after remaining on the surface for a while. This observation supports the view regarding pit nucleation in aluminum offered by Bargeron and Givens.[4] They found that blistering occurred along the oxide/metal interface and resulted in breaking of the film because of high hydrogen gas pressure created in blisters, which therefore acted as precursors of pits.

The data shown in Fig. 3 also indicated that no appreciable frequency effect was identified at frequencies between 5 and 20 Hz. However, it is probable that lower frequencies would have a significant effect. This aspect is under further study. In addition, the life to detection of a corrosion pit is hardly affected by stress levels between 79 and 89 MPa. The average pit detection life was about 35% of total corrosion fatigue life.

Final Failure

An S/N plot of maximum fatigue stress versus cycles to failure is shown in Fig. 5. Only the results of the specimens tested in 3.5% NaCl solution are shown in this plot. The specimen tested in laboratory air at a stress level of 80 MPa ran out at 7,811,500 cycles, which is the highest number of cycles of survival for all tested specimens. For comparison, some of the results presented by Antolovich and Saxena [5] are also shown in Fig. 5. These results are from specimens of 7075-T6 aluminum alloy that were tested in laboratory air. Cracks nucleated at the corners of the specimen in all cases and the detectable crack size for the nucleation was about 0.4 mm. Since the period between crack detection and final failure was only several thousand cycles, it was difficult to observe crack propagation during testing. Therefore, the effect of environment is considered to contribute mainly to the fatigue crack nucleation and early propagation processes. Additional studies of this aspect also are underway. It should be mentioned here that the life spent to detect the fatigue crack means the life from the beginning of the experiment until the detection of a 0.4 mm crack. The detection of the crack at a length of 0.4 mm includes the pit nucleation and growth stages as well as crack formation at the pits plus some growth. Clearly, to completely model this process additional detailed studies are needed. Indeed, portions of these studies are underway.

As shown in Fig. 5, a 3.5% NaCl environment lowers about 60% the fatigue strength of aluminum 7075-T6 specimens. For these conditions, since corrosion pits were found on the exposed surfaces of

almost all specimens tested in 3.5% NaCl solution and the specimen tested in laboratory air did not fail at the same stress level, it is believed that the pits provide local stress concentrations that accelerate fatigue crack nucleation and reduce fatigue life of 7075-T6 material. In addition, we observed intergranular cracks in the pits. These also may play a significant role in nucleating the fatigue cracks. As expected, the lower frequency (5 Hz) reduces the fatigue life a slight amount compared to the higher frequency (20 Hz). The reason is because low frequency allows more time for corrosion reactions to occur. Additional studies of the effect of frequency and variable amplitude loading cycles are underway within Quality and Integrity Design Engineering Center in the Mechanical Engineering Department at the University of Utah.

METALLOGRAPHIC INVESTIGATION

In order to evaluate the effect of the microstructure on pitting corrosion fatigue behavior of 7075-T6 aluminum alloy, a metallographic examination was conducted on specimens tested in 3.5% NaCl solution using an optical stereo microscope.

Profiles of adjacent cross sections of a tested specimen are shown in Fig. 6. To produce these adjacent cross sections, a vertical section was made through preselected pits and they were photographed. Then more material was removed from the specimen and the corrosion pits again were photographed . This process was repeated a third time. It is evident that the three pits shown in Fig. 6 (a) have coalesced. After removing a layer of metal from the pit cross section, it can be seen that the same pits were separate and had varied shapes and sizes, Fig. 6 (b). It is obvious that discrete pits nucleated at first, but that with increasing exposure time, pit coalescence took place to cause more extensive local attack. The same phenomenon was observed by Baker [6] when he studied the corrosion resistance of aluminum-magnesium-silicon alloy under a salt-spray condition.

According to ASTM standard G 46-76 (Standard practice for Examination and Evaluation of Pitting Corrosion), the pits shown in Fig. 6 (a) and (b) appear in the elliptical shape except for the smaller one in Fig. 6 which shows the narrow and deep shape. To evaluate the cross-sectional shapes of the same pits in more detail, another layer of the pit cross section was removed and the resulting pit shapes are shown in Fig. 6 (c). It is interesting to note that two pits joined together under the surface showing the undercutting shape with different depths, and other pits exhibited intergranular attack which originated from the base of the pit. Therefore, it can be concluded that a pit shape may vary irregularly when growing and it is difficult to determine the true maximum pit depth by the method of cross-sectioning the pit because the deepest pit may not have been selected and the pit may not been sectioned at the deepest point of the penetration. This observation provides evidence that modeling the pits will be an extremely complex process. Perchance on equivalent initial flaw size approach will be the best we can do. Modeling studies have been underway [1,2] by the first author and they are continuing under this program.

Further evidence of intergranular corrosion occurring along with the pit, in which case intergranular fissures advance into the metal laterally from the pit cavity, was identified on the exposed surface of another specimen after polishing and etching. Fig. 7 shows that the cracks which nucleated from the pit on the exposed surface of the specimen were caused by intergranular corrosion attack. In both cases (Figs. 6 (c) and 7) intergranular cracking originated from the pit. The reason for this might be that the electrochemical conditions in the pit readily lead to the occurrence of intergranular attack. According to Lifka,[7] in high-strength aluminum alloys the susceptibility to intergranular attack results from a localized decomposition of a solid solution at the grain boundaries and the formation of a precipitation in the vicinity of the grain boundaries. In the case of 7075-T6 aluminum, intergranular corrosion is probably related to the precipitation of the grain boundary phases, such as $MgZn_2$, which may themselves behave anodically with respect to the adjacent alloy. Hence, it is reasonable to believe that intergranular corrosion is another corrosion mechanism involved in crack nucleation in this research. Additionally, since the intergranular corrosion was found to penetrate deeply into the metal leaving behind little visible evidence of damage (Fig. 8), it is possible that intergranular corrosion may cause failure with extreme suddenness, especially when the materials are subjected to a lower fatigue stress level and a longer exposure time than in the present testing.

This observation provides evidence for the great concern that pit formation and growth, accompanied by intergranular attack may lead to degradation of integrity. In this case, based on the metallographic examination and the observation during testing, pitting seems the predominant corrosion attack mechanism. This observation has potential significance in relation to modeling the corrosion pitting fatigue process.

It also is noted that pit growth was strongly dependent on the orientation with respect to the rolling direction of the material as shown in Fig. 6. The same phenomenon was found in the other specimens. Fig. 8 presents the pits on the exposed surface of a different specimen. The picture shows that severe attack occurred along the fibrous grain orientation in the rolling direction.

FRACTOGRAPHIC INVESTIGATION

A fractographic examination of the specimen fracture surfaces was conducted using scanning electron microscopy. This was done to confirm the notion, based on this and other experimental work, that has demonstrated that pits have been considered to be the cause of accelerated fatigue crack nucleation with a concomitant reduction in fatigue life. As well, the fractography was done to provide additional insight into the mechanisms involved in the pitting corrosion fatigue phenomenon. This investigation included two steps. First, the fracture surfaces were examined to study the origin of fracture and fracture modes involved in the fracture processes. Second, the exposed surfaces, which were related to the fracture, were examined to deal with the corrosion damage.

Fracture Surface Examination

By tracing the radial track surface features shown in Fig. 9 it is evident that the fatigue cracks originated at the sites of corner corrosion pits. This observation confirms the assumption that the corrosion pits acted as stress concentration sites which resulted in nucleation of fatigue cracks. Careful examination around the crack nucleation areas showed that corner pits at the origin sites nucleated in the areas close to the corner of the edge surfaces which were covered with coating broken by solution penetrating during testing. The observations for the other specimens also indicated that the corner pits and pits close to the corners were preferential sites for fatigue crack nucleation. The reason for the evident preference for the crack to start at the corner pits or the pits close to the corners could be explained by the fact that the curved edges of the specimens were the most highly stressed areas compared to the other areas in the specimens. Finite element analysis confirmed this and is to be reported elsewhere. Some small pits also were found on the fracture surface, Fig. 9. However, it is obvious that crack nucleation was dominated by the large corner corrosion pit. It is recognized that in other cases the multiple damage sites (pits) away from the corners nucleate cracks that link up. This has been reported in other work by Hoeppner.[2]

One interesting phenomenon noticed was that the fatigue cracks seem to nucleate from the bottoms of the pits, Fig. 9. Some research [8] showed that a growing pit is a local electrochemical cell. The bottom of the pit is the anode and the surrounding walls of the pit and surface of the metal are the cathode. The fatigue crack nucleation occurred at the bottom of the corrosion pit, probably because this place is electrochemically active and the stress concentration is large enough to lead to the crack. Therefore, it is natural to conclude that corrosion fatigue nucleation is controlled by the rate at which pits nucleate and grow to a critical depth and shape. This interpretation must be tempered by the observation of integranular cracking as discussed above.

Most of the fracture surface was the fatigue crack propagation region where transgranular fracture was found to be the primary fracture path. Fig. 10 shows cleavage-like fracture, with river patterns emanating from the origin in the area adjacent to the fracture origin (see also Fig. 11). A small corrosion pit appeared on the surface, but no indication of the intergranular decohesion which would be the result of the intergranular corrosion was observed during the metallographic examination. Similar features were seen in

specimens tested in air from the literature.[9] Observation of the fracture surface also shows little ductility in that the cleavage facets with a few dimples appeared in the crack propagation region, Fig. 11. This phenomenon was observed repeatedly. Although crack propagation did involve other mechanisms, "quasi-cleavage" was found to be the primary mechanism for 7075-T6 aluminum tested in 3.5% solution under cyclic loading.

Away from the fatigue crack nucleation sites, well-defined fatigue striations were found in the crack propagation region, Fig. 12. This feature was observed in most specimens examined. No evidence of environmental influence was identified after the crack became long enough. This corresponds to the observation from the experimental work, in which crack propagation was too fast (only several thousand cycles taken in the crack propagation stage) to allow the chemical reaction to occur. Also, this is consistent with many observations in this field. Separate studies of the role of environments on fatigue crack propagation have been done by the second author and others and also are currently underway as part of this overall program.

Exposed Surface Examination

Numerous small and shallow cavities were observed on the exposed surface as shown in Fig. 13. These cavities were the result of the local breakdown of protective films and presumably attack at constituent particles and act as precursors of pits. Relatively large and deep corrosion pits also were found on the exposed surfaces of the specimens. These pits were distributed randomly on the exposed surfaces and appeared in different shapes and sizes. Figs. 14 and 15 show the appearance of pits observed in one specimen. It was interesting to notice that these pits had different shapes on the same exposed surface. Fig. 14 shows a typical hemispherical pit located at near center of the exposed surface. A group of pits was found on the same exposed surface as shown in Fig. 15, which exhibits multi-site damage (MSD) related to corrosion pitting. This group of the pits showed coalescence of pits giving rise to more local attack, and these pits appeared in irregular shapes. Numerous pits in a group also were observed in the other specimen as shown in Fig. 16. Pits in this group grew along the orientation with respect to the rolling direction of the material. All the pits were three dimensional in nature. The shapes of the corrosion pits might influence the fatigue life in different degrees, since the magnitude of the stress concentrations depends on the pit shape and geometry dimensions.

Pits created on the exposed surfaces generally showed the sharp edges that are believed to be caused by crystallographic corrosion tunneling, Fig. 17. A micro-crack also was observed at the pit edge in this figure. Furthermore, the walls of pits were found to be rough. The crack-like sharp corners and the rough sites inside a pit should increase the local stress concentration and play an important role in the fatigue life of the material.

CONCLUSIONS

The following conclusions are drawn from this study:

1. Corrosion pits, especially corner corrosion pits, were responsible for fatigue crack nucleation of 7075-T6 aluminum specimens tested in 3.5% NaCl solution. The fatigue life was found to be strongly dependent on pit formation and growth.

2. The fatigue strength of 7075-T6 aluminum tested in 3.5% NaCl solution was reduced by about 60% compared with that tested in laboratory air. The latter data were obtained from the literature. It is believed that the reason is the corrosion pits act as the sites of stress concentration to accelerate fatigue crack nucleation and also produce intergranular cracks.

3. No appreciable frequency effect was observed in the pit nucleation process for the frequencies tested in this work. However, this parameter was found to have an effect on total corrosion fatigue life. It is believed that reduction of fatigue life at low frequency was associated with a greater corrosion effect on promoting the pit growth rate than at high frequency.

4. Pits appeared in various morphologies and were three-dimensional in nature. It was found that pits had rough internal walls and crack-like sharp edges. These crack-like sharp edges and rough pit walls were considered to cause higher stress concentrations and to readily nucleate the fatigue crack, leading to the reduction of the fatigue life.

5. The growth of the pits depends strongly on the orientation of the grain with respect to the microstructure and crystallographic orientation of the material.

6. Intergranular corrosion cracks were found along with pitting, suggesting that intergranular attack might lead to fatigue cracking.

7. The mechanism governing the propagation of the fatigue cracks originating at corrosion pits was "quasi-cleavage".

FUTURE STUDIES

This research is a small part of an extensive activity on pitting corrosion fatigue dating back to 1965. Additional detailed studies are underway and planned related to those reported herein as follows:

(1) Fracture mechanics based modeling activities.

(2) Frequency and load spectrum effects.

(3) Effect of aircraft environments. This activity involves sampling aircraft environments at aircraft maintenance and overhaul activities.

(4) Additional studies of pit characterization.

(5) Statistically planned experiments for more reliable evaluation of some of the early observations.

(6) Corrosion pitting studies with other aluminum and titanium alloys.

REFERENCES

1. Hoeppner, D.W.: Corrosion Fatigue Considerations in Materials Selections and Engineering Design. *Corrosion Fatigue: Chemistry Mechanics and Microstructure*, O. Devereux, A.J. McEvily, R.W. Staehle, Ed., NACE-2, National Association of Corrosion Engineers, 1972.

2. Hoeppner, D.W.: Model for Prediction of Fatigue Lives Based Upon a Pitting Corrosion Fatigue Process. *Fatigue Mechanisms*, Proceedings of an ASTM-NBS-NSF Symposium, J.T. Fong, Ed., ASTM STP 675, American Society for Testing and Materials, 1979.

3. Cox, J.M.: Pitting and Fatigue-Crack Initiation of 2124-T851 Aluminum in 3.5% NaCl Solution. *M.S. Thesis*, University of Missouri-Columbia, 1979.

4. Bargeron, C.B.; and Givens, R.B.: Source of Oscillations in the Anode Current during the Potentionatatic Pitting of Aluminum. *Electrochemical Society Journal,* Vol.124, 1977, pp.1230-1232.

5. Antolovich, S.D.; and Saxena, A.: Fatigue Testing. *Metals Handbook,* 9th Edition, Vol.8, ASM International, Metals Park, Ohio, 1985, p.364.

6. Baker, S.V.; Lyon, S.B.; Thompson, G.E.; Wood, G.C.; and Lewis, K.G.: A Comparison of Potentiodynamic Polarization Tests with Wet-dry Mixed Salt-Spray Testing of Aluminum-Magnesium-Silicon Alloy. *New Methods for Corrosion Testing of Aluminum Alloys,* ASTM STP 1134, Philadelphia, 1992, pp.32-49.

7. Lifka, B.W.; and Sprowls, D.O.: Significance of Intergranular Corrosion in High-Strength Aluminum Alloy Products. *Localized Corrosion - Cause of Metal Failure,* ASTM STP 516, 1972, pp.120-144.

8. Payer; J.H.; and Staehle, R.W.: Localized Attack on Metal Surface. *Corrosion fatigue: Chemistry, Mechanics and Microstructure,* National Association of Corrosion Engineers, 1972, pp. 211-218.

9. Kerlins, V.: Modes of Fracture. *Metals Handbook,* 9th Edition, Vol.12, ASM International, Metals Park, Ohio, 1987, p.54.

ACKNOWLEDGMENTS

The authors would like to thank the Boeing Commercial Airplane Company for providing financial support for this study. The authors also are grateful to the staff at the Quality and Integrity Design Engineering Center in the Department of Mechanical Engineering at the University of Utah for assistance with experimental work. This effort is part of an effort on studies on environmental effects on fatigue behavior of aircraft structural materials.

Table 1. Mechanical properties of 7075-T6 aluminum alloy

Yield strength (MPa)	Ultimate strength (MPa)	Elongation (%)	Modulus of elasticity (MPa x 10^3)
503	572	11	72

Table 2. Chemical composition of 7075-T6 aluminum alloy, wt%

Cu	Mg	Zn	Cr	Al
1.6	2.5	5.6	0.3	Balance

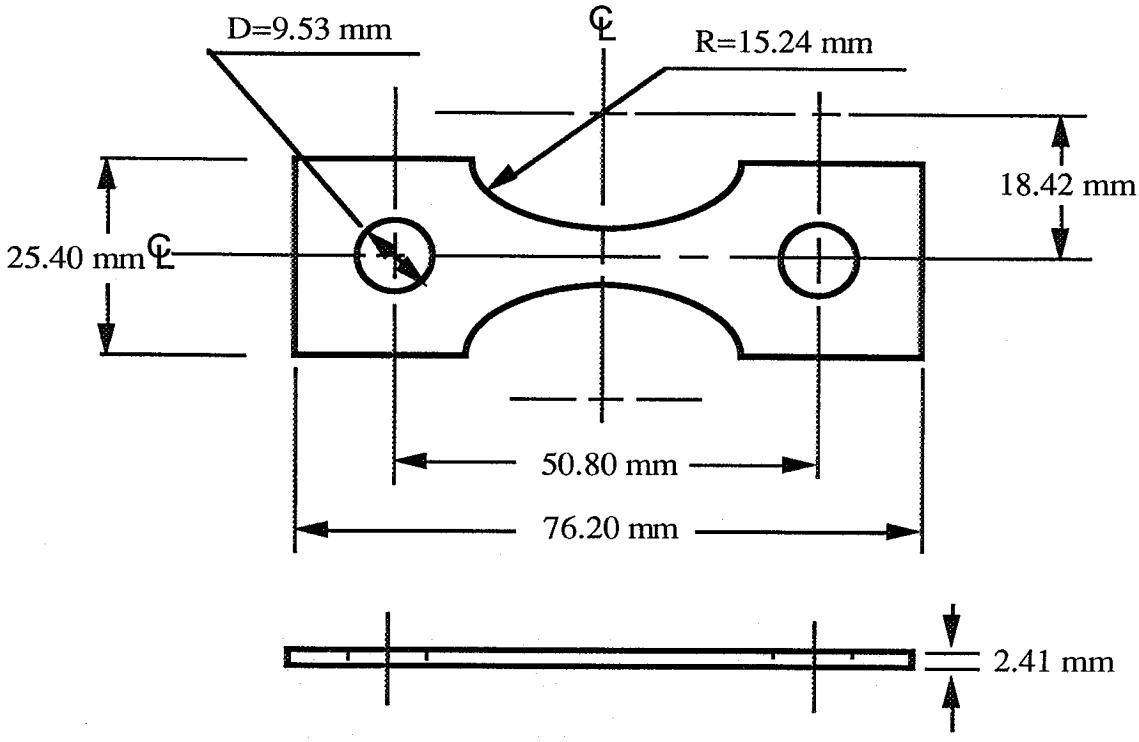

Fig. 1. Unnotched specimen.

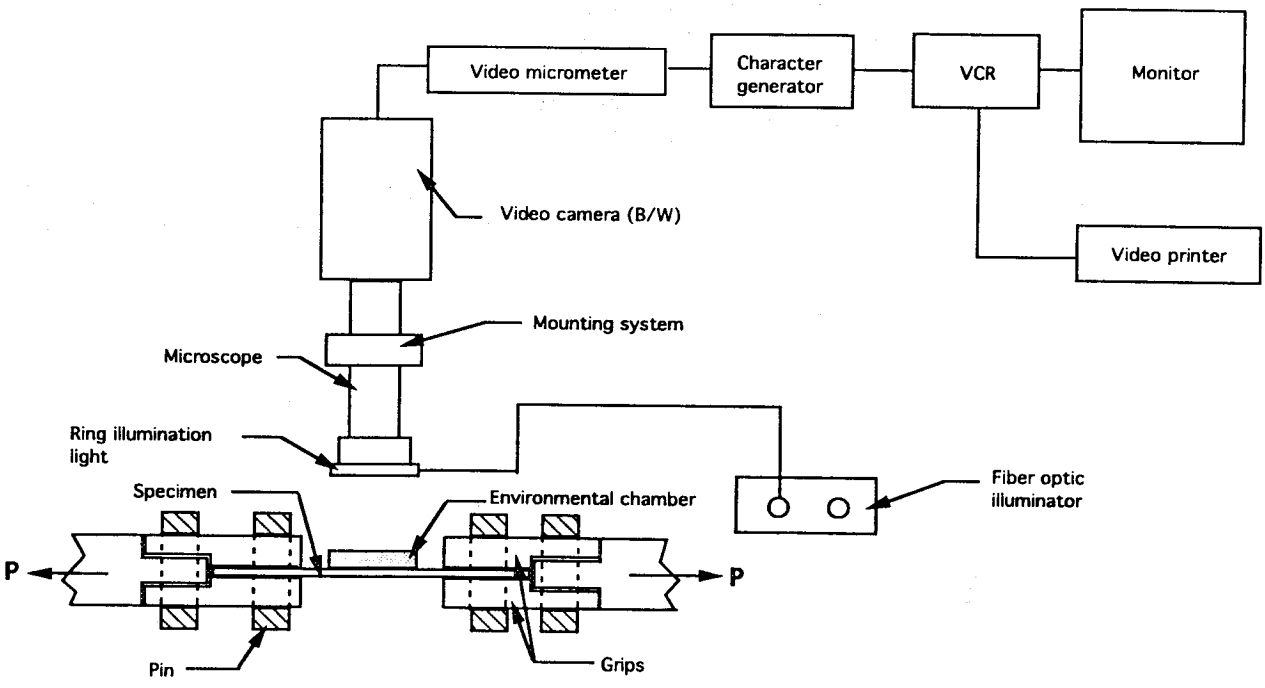

Fig. 2. Schematic diagram of recording system and specimen mounted in grips.

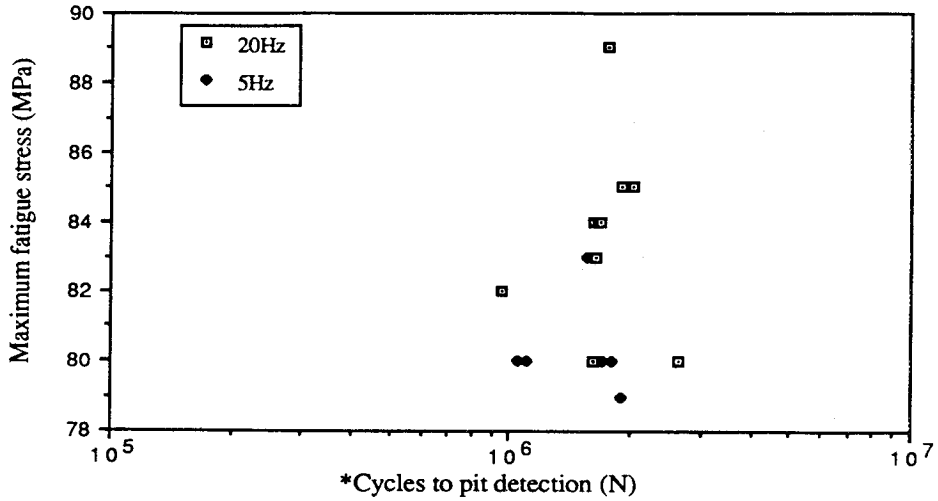

Fig. 3. Stress Vs. life plot of pit detection data.
* Cycles to pit detection means the cycles at which the "first pit" was observed at the length of about 0.02 mm. Thus, this length includes pit nucleation plus some growth.

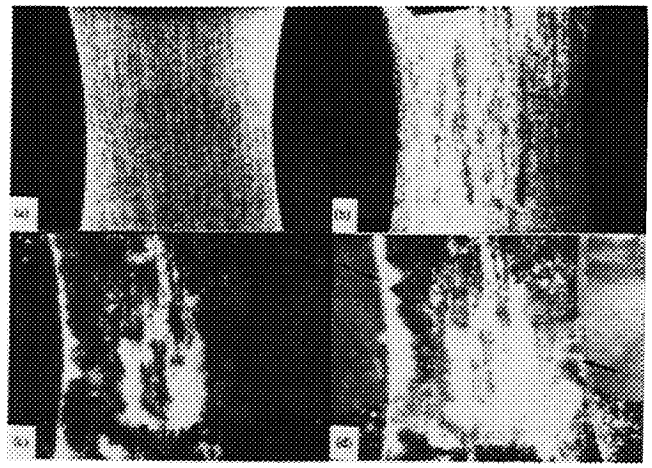

Fig. 4. Video images of changes in surface states of the specimen in 3.5% NaCl, magnification 10.5X, (a) cycle, N=0, (b) cycles, N=68,900, (c) cycles, N=828,000, (d) cycles, N=3,082,000. Arrows indicate pits.

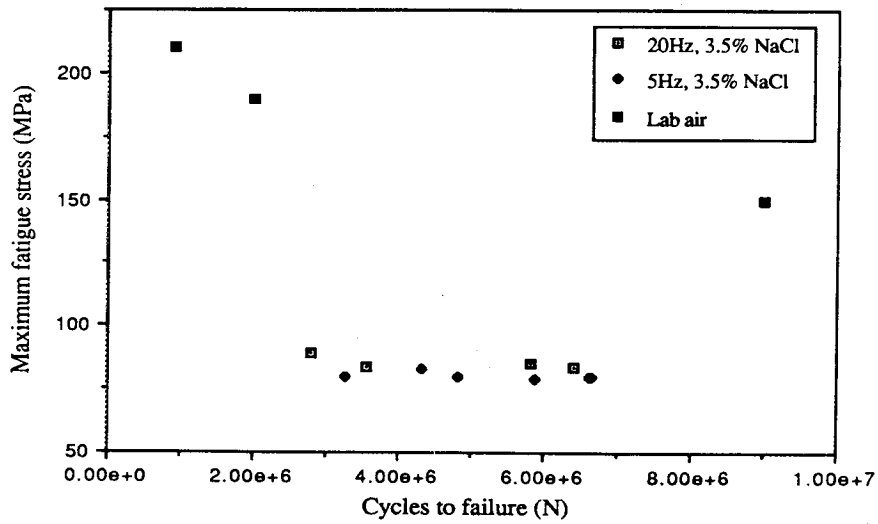

Fig. 5. Plot of maximum stress vs. number of cycles to failure for pitting corrosion fatigue tests. Lab air data[2] is used for comparison.

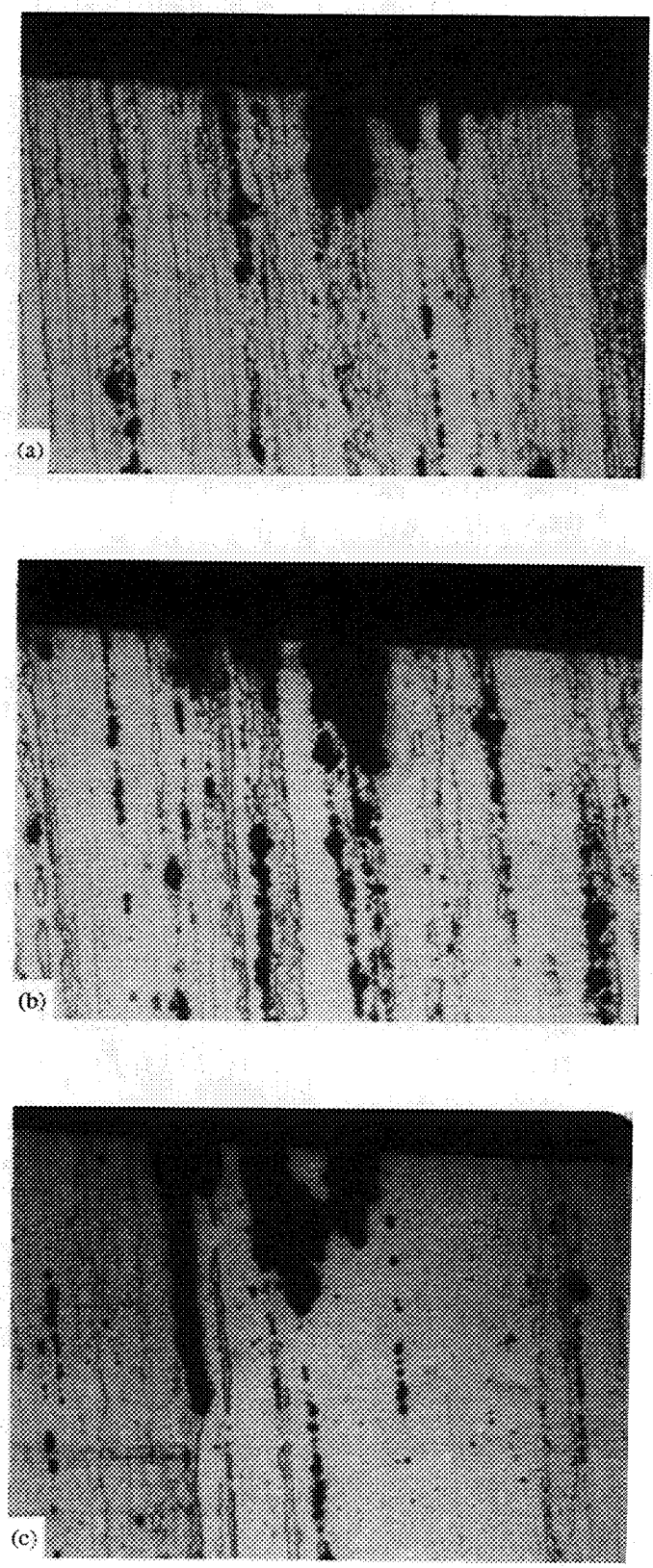

Fig. 6. Cross section of pits in the specimen tested in 3.5% NaCl solution, magnification 400X (reproduced by 320 magnification), (a) after cross-sectioning, (b) after removing a layer of metal, (c) after removing the second layer of metal.

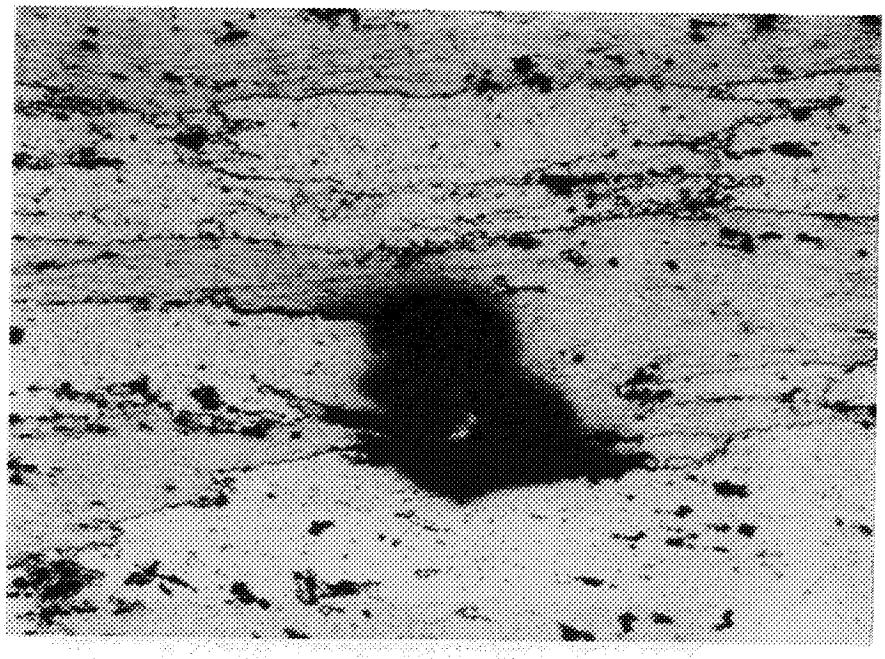

Fig. 7. Corrosion pit along with the intergranular corrosion cracks on the exposed surface of the specimen tested in 3.5% NaCl solution, magnification 200X. Arrows indicate the loading directions.

Fig. 8. Corrosion pits on the exposed surface of the specimen showing pit growth in the rolling direction, magnification 100X.

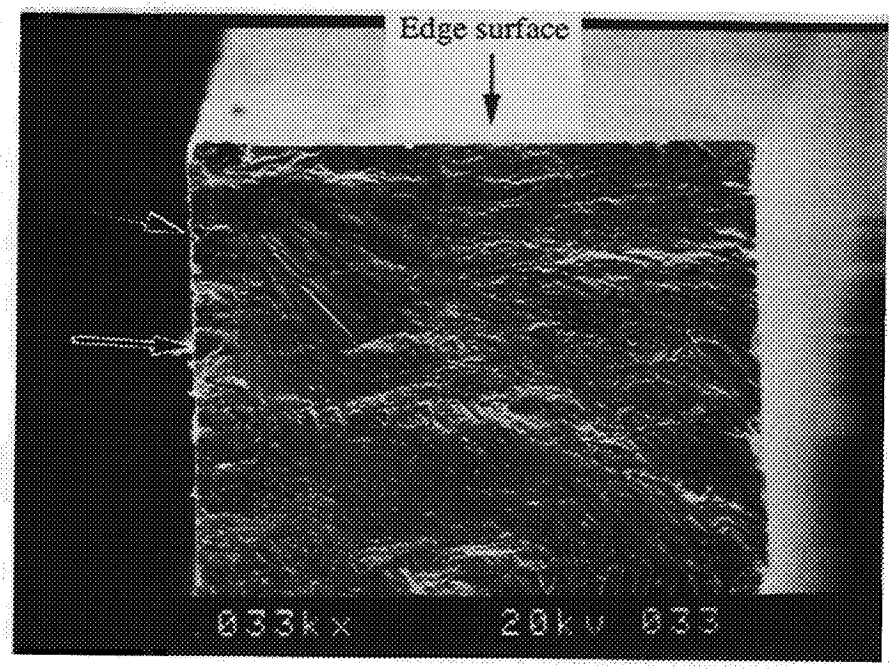

Fig. 9. The crack nucleation area of the specimen tested in 3.5% NaCl solution showing the fracture origin at a corrosion pit. Arrows indicate the exposed surface and a small pit.

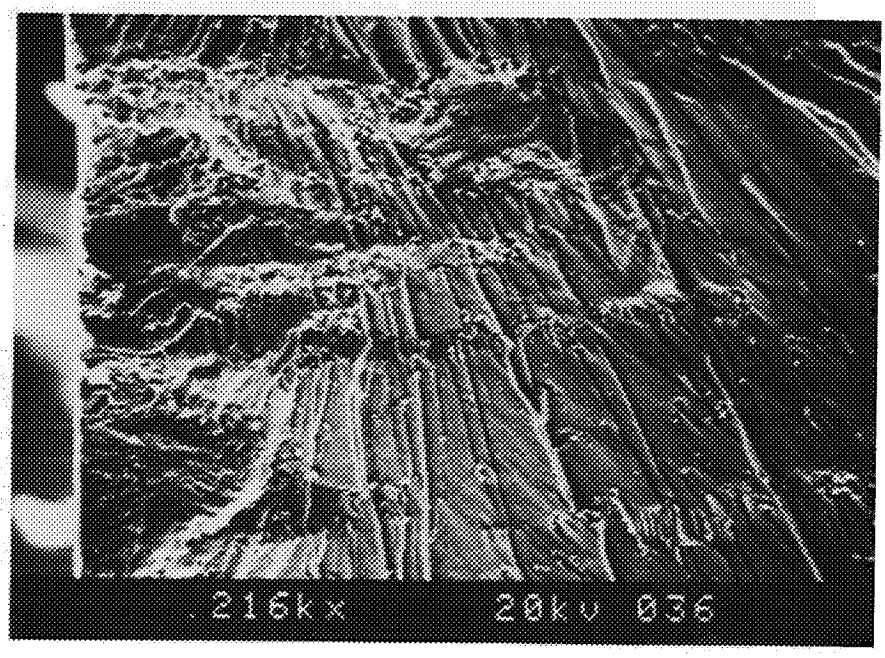

Fig. 10. Cleavage-like fracture near the crack origin of the same specimen showing in Fig. 9.

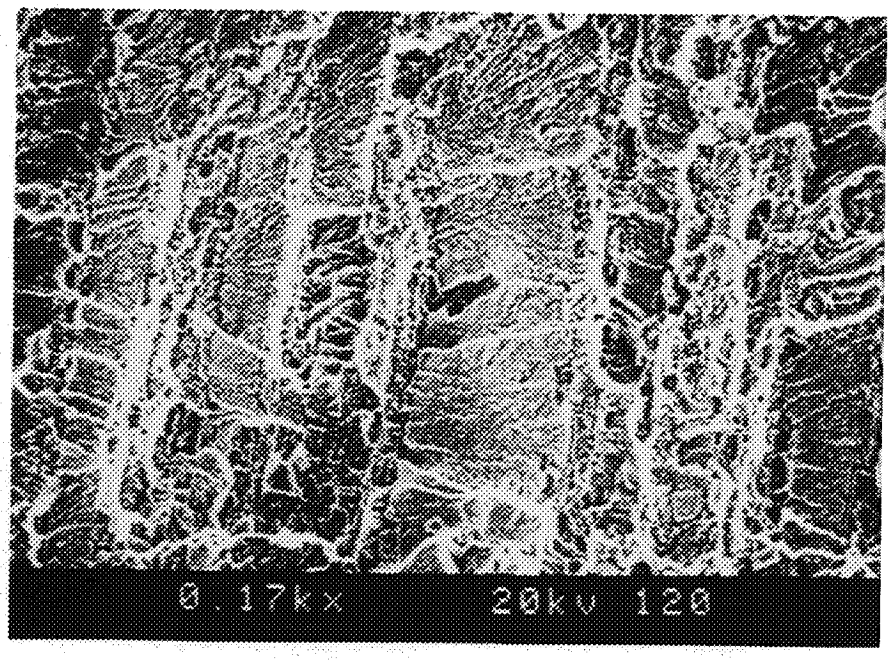

Fig. 11. Cleavage facets with a few dimples in the crack propagation area of the specimen tested in 3.5% NaCl solution.

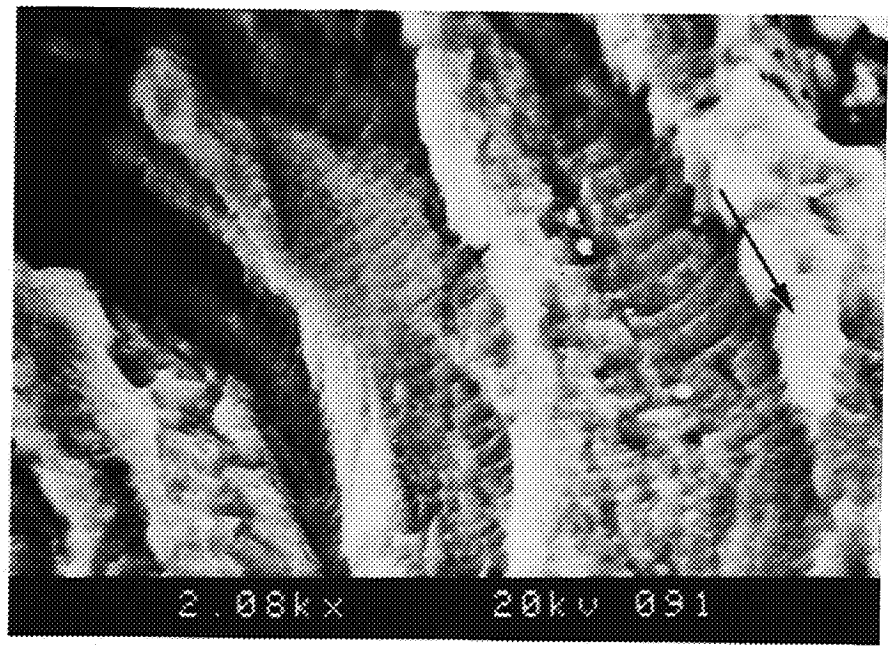

Fig. 12. Fatigue striations in the crack propagation area of the specimen tested in 3.5% NaCl solution. Arrow indicates the crack propagation direction.

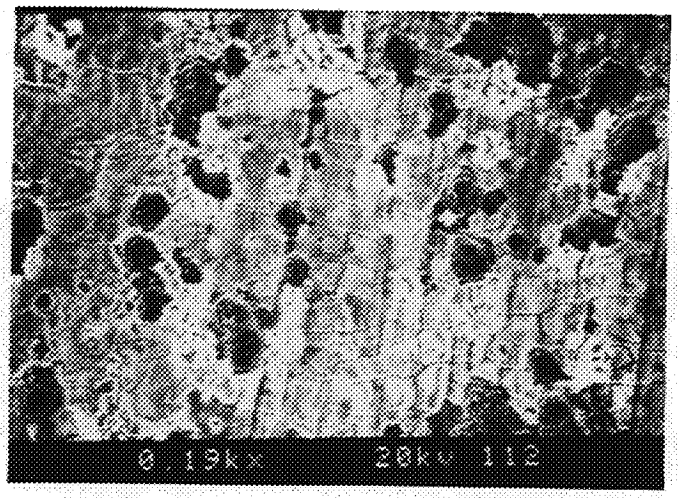

Fig. 13. Small cavities on the exposed surface of the specimen tested in 3.5% NaCl solution (cycles to failure are 4,822,200).

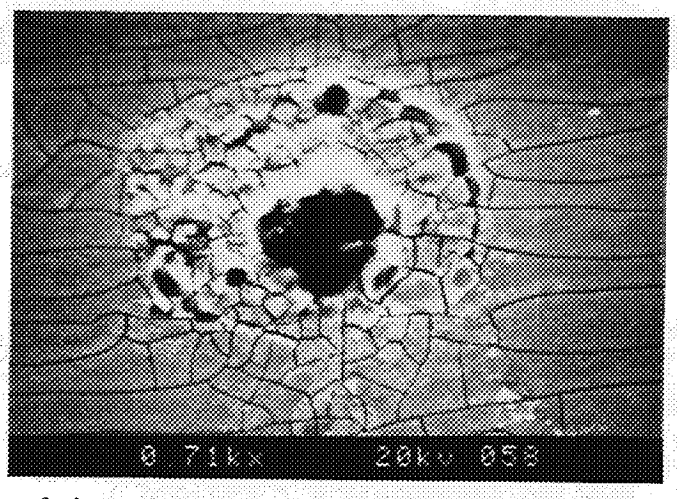

Fig. 14. Hemispherical shape of pit on the exposed surface of the specimen tested in 3.5% NaCl solution (cycles to failure are 3,279,300).

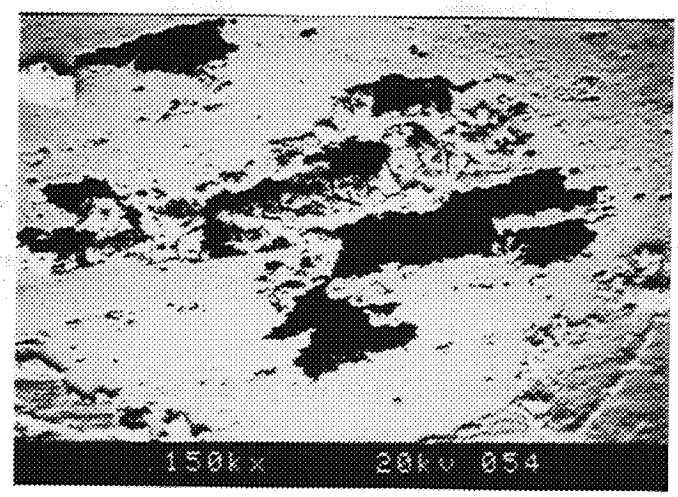

Fig. 15. Group of pits on the same specimen showing in Fig. 14.

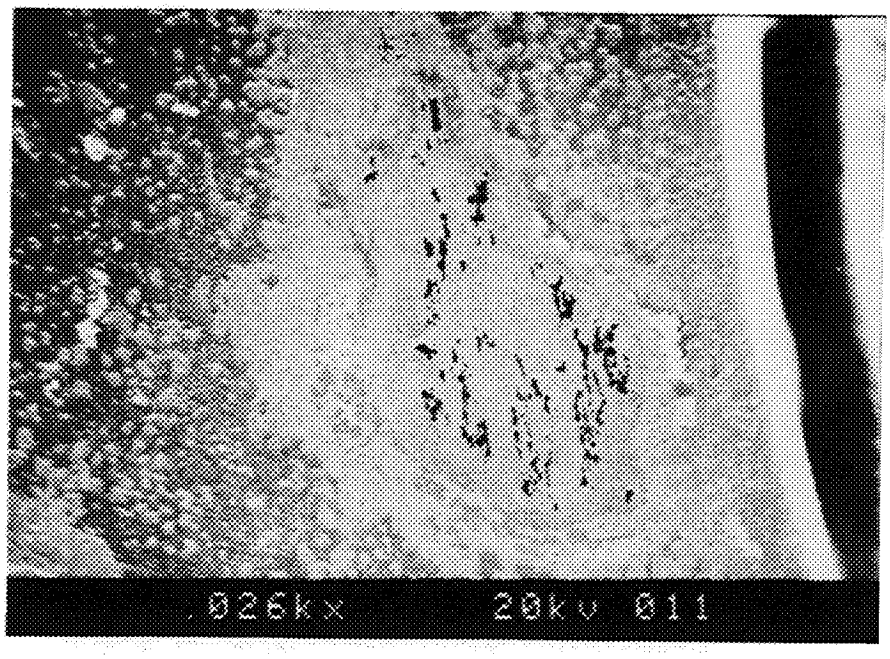

Fig. 16. Pits appear in a group in the specimen tested in 3.5% NaCl solution.

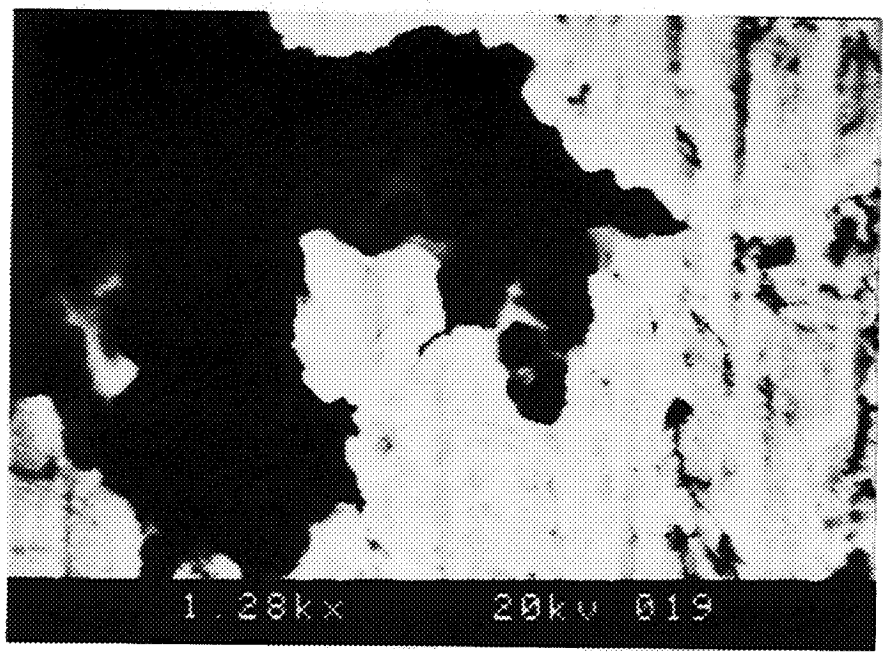

Fig. 17. Part of the pit showing the sharp edges of the pit and the microcrack at the pit in the specimen tested in 3.5% NaCl solution.